# Co-diet supplementation of low density polyethylene and honeybee wax did not influence the core gut bacteria and associated enzymes of *Galleria mellonella* larvae (Lepidoptera: Pyralidae)

*Grégoire Noël[1], Laurent Serteyn[1], Abdoul Razack Sare[2], Sébastien Massart[2], Frank Delvigne[3], Frédéric Francis[1]*

**Author affiliations**

[1] Functional and Evolutionary Entomology, TERRA Teaching and Research Centre, Gembloux Agro-Bio Tech, University of Liège, Gembloux, Belgium

[2] Integrated and Urban Plant Pathology Laboratory, TERRA Teaching and Research Centre, Gembloux Agro-Bio Tech, University of Liège, Gembloux, Belgium

[3] Laboratory of Microbial Processes and Interactions, CARE FoodisLife, TERRA Teaching and Research Centre, Gembloux Agro-Bio Tech, University of Liege, Gembloux, Belgium

**Corresponding author**

gregoire.noel@uliege.be

**ORCID number**

Grégoire Noël : 0000-0001-5994-1022

Laurent Serteyn : 0000-0001-6036-3864

Abdoul Razack Sare : 0000-0002-0941-1901

Frank Delvigne : 0000-0002-1679-1914

Frédéric Francis : 0000-0001-7731-0849

**Acknowledgment**

We thank to Samuel Latour for his work. We thank Nicolas Poncelet (ULiège) for experimental assistance. We thank also Dr. Dominique Baiwir and Dr. Gabriel Mazzucchelli of GIGA-Proteomics team (ULiège) (https://www.gigaproteomics.uliege.be/cms/c_4214690/en/gigaproteo) that directed the protein sequencing. We also thank Hillary Fischer (ULiège), a native English speaker, for proof reading the manuscript.

**Abstract**

The current plastic pollution throughout the world is a rising concern that demands the optimization of biodegradation processes. One avenue for this is to identify plastic-degrading bacteria and associated enzymes from the gut bacteria of insect models such as *Tenebrio molitor*, *Plodia interpunctella* or *Galleria mellonella* that have the ability to ingest and rapidly degrade polyethylene. Therefore, this study takes part in understanding the role of the gut bacteria by investigating *G. mellonella* as a biological model feeding with a diet based on honeybee wax mixed or not with low-density polyethylene. Gut microbiome was analyzed by high throughput 16S rRNA sequencing, and *Enterococcaceae* and *Oxalobacteraceae* were found to be the major bacterial families. Compared to the control, the supplementation of low-density polyethylene did not cause significant modification of the bacterial microbiota at community and taxa levels, suggesting bacterial microbiome resilience. The bacterial proteome analysis of gut contents was encouraging for the identification of plastic degrading enzymes such as the phenylacetaldehyde dehydrogenase which participate in styrene degradation. This study allowed a better characterization of the gut bacteria of *G. mellonella* and provided a basis for the further study of biodegradation of polyethylene based on the bacterial microbiota from insect guts.

**Keywords:** great wax moth, insect gut microbiome, plastic biodegradation, plastic degrading enzymes, insect larvae

## 1. Introduction

The current plastic wastes pollution throughout the world is a serious issue. Synthetic plastics like low-density polyethylene (PE) are used to produce packages intended for many industrial sectors such as food, pharmaceutical, cosmetics, detergent or chemical (Shimao 2001). In 2020, worldwide production of plastic reached 367 megatons (Plastics Europe 2021). Indeed, its physicochemical properties made plastic a standard material in many fields. Properties such as hardness, effectiveness and cost are suitable for industries (Ojha et al. 2017). However, these synthetic materials have the inherent characteristic to persist in natural ecosystems in a detrimental way and more than forty years ago even, researchers identified a worrying amount of plastic particles drifting in the ocean (Carpenter and Smith 1972). Hence, impacts of micro- and macro-plastics on terrestrial and marine environment are being addressed (Li et al. 2016).

In order to reduce this pollution, research during the last decades has endeavored to enhance the degradation pathway of plastic wastes like PE. However, the high molecular weights, as well as the linear carbon structure of this polymer, prevent an easy and fast degradation process. Abiotic factors like heating or UV exposure allow an effective pre-ageing for a subsequent biodegradation (Bonhomme et al. 2003; Kundungal et al. 2021). However, a promising aspect of weathering plastic wastes is the colonization by a panel of microbial colonies, typically forming biofilms on the surface (Koutny et al. 2006; Oberbeckmann et al. 2016; Ghatge et al. 2020), that can expedite the biodegradation of the plastics. Several microorganisms have been investigated which take part in the different steps of the biological degradation of polymers (Ghatge et al. 2020). First, bio-deterioration modifies the physical and chemical properties and the size of the polymer is then reduced by enzymatic fragmentation. Then, assimilation and mineralization allow the conversion of its molecules by metabolism (Ojha et al. 2017). However, the process of plastic biodegradation by isolated bacterial populations may take years. Additionally, higher level organisms like insects also have the ability to participate in plastic biodegradation processes (reviewed in Pivato et al. 2022). Among them, *Tenebrio molitor* (Coleoptera: Tenebrionidae) (L. 1758), *Plodia interpunctella* (Lepidoptera: Pyralidae) (Hübner 1813), *Achroia grisella* (Lepidoptera: Pyralidae) (Fabricius 1794), the greater wax moth *Galleria mellonella* (Lepidoptera: Pyralidae) (L. 1758) are valuable candidates (Yang et al. 2014, 2015; Bombelli et al. 2017; Brandon et al. 2018; Kundungal et al. 2019). Recently, effects of PE or other plastic wastes on the bacterial gut microbiome of *G. mellonella* larvae have been highlighted,

suggesting that this species can adapt its microbiome for the degradation of plastic with associated bacterial lineages (Cassone et al. 2020; Lou et al. 2020; Zhu et al. 2021) although further investigations are required to identify and understand more deeply the gut bacterial communities favored by the plastic diet. Indeed, *G. mellonella* is an insect pest of apiaries whose larvae voraciously feed on honeycomb before pupation when honeybee colonies are weak, especially at the end of their foraging season (Kwadha et al. 2017). Since PE is chemically related to the wax produced by the honeybees (Dadd 1966), this suggests that the greater wax moth larvae have potentially the physical and biochemical machinery to metabolize the PE. Even if some studies suggested a particular role of *G. mellonella* gut microbiome, gut epithelial cells or proteins secreted by the salivary glands (Kong et al. 2019; Cassone et al. 2020; Peydaei et al. 2020, 2021; Lou et al. 2020; LeMoine et al. 2020), the biological mechanisms involved in the metabolism of PE by *G. mellonella* gut can be deepened (Kumar Sen and Raut 2015; Ghatge et al. 2020; Mohanan et al. 2020; Amobonye et al. 2021; Sanchez-Hernandez 2021). Furthermore, the exploration of the bacterial gut microbiome of *G. mellonella* showed composition changes after consumption of PE (Cassone et al. 2020; Lou et al. 2020); it included potential candidates for plastic biodegradation such as *Serratia*, *Bacillus*, *Acenitobacter*, *Desulfovibrio Lactobacillus*, *Pseudomonas* and *Enterobacter* lineages (Cassone et al. 2020; Lou et al. 2020; Peydaei et al. 2021; Ruiz Barrionuevo et al. 2022). Nevertheless, the influence of PE on gut microbiome of *G. mellonella* remains patchy as these studies diverged in their results of bacterial association with PE. Therefore, additional studies could be investigated to strengthen the survey of *G. mellonella* gut microbiome in order to identify new and/or known plastic-eater bacteria (Montazer et al. 2020) and to also improve the understanding of the plastic biodegradation pathway.

High-throughput sequencing allows a better understanding of microbial communities (Jovel et al. 2016). Sequencing of the 16S rRNA gene is a gold standard for taxonomic studies. In this study, Illumina sequencing of partial 16s rRNA sequence was applied to show the effect of plastic consumption on the midgut-hindgut bacterial microbiota of the greater wax moth caterpillars, *G. mellonella* (Lepidoptera: Pyralidae). Indeed, the main digestive processes occur in the midgut of insect. Bacteria play a vital role in degrading organic matter, a great proportion of the digestive enzymes are released in this gut segment while the hindgut usually corresponds to the absorption of water and formation of excrements (Engel and Moran 2013; Stefanini 2018). However, the hindgut may also harbor specific bacterial communities such as a ring-

shaped biofilm of the moth *Hyles euphorbiae* (L.) or bacteria involved in the cellulose and xylan hydrolysis for wood-feeding termites *Nasutitermes ephratae* (Holmgren 1910) and *N. corniger* (Motschulsky 1855) species (Warnecke et al. 2007; Vilanova et al. 2016). *G. mellonella* is generally considered as an insect model for pathogenic experimentation (especially for human pathogens; e.g. in Sugeçti 2021a or in Sugeçti 2021b) by its by its ease of mass rearing, ease of larval manipulation and its metabolic similarities with vertebrate immune system (Cook and McArthur 2013; Jorjão et al. 2017; Dinh et al. 2021). Identifying bacteria just through metagenomics cannot infer on the metabolic pathway that could be favor by the adding of PE in the larval diet. Metaproteomics can fill this gap by identifying which proteins are observable and under what conditions (Petriz and Franco 2017). Thus, the combined information of gut bacteria community and its associated proteome may be investigated as an opportunity to deepen our knowledges in the biodegradation of PE. To date, little is known about plastic degrading enzymes, especially from gut bacteria of insects. Through molecular signatures with RNAseq analysis and quantification of total lipid content, one recent study found enhanced fatty acid metabolism and lipid oxidation activity of the gut cells for *G. mellonella* larvae fed with PE (LeMoine et al. 2020). Furthermore, some alkane hydroxylases isolated from bacteria have a complementary pivotal role (regarding the gut cells) to hydrolyze the PE alkanes and release primary and secondary alcohols (Kong et al. 2019). Therefore, the digestive tract of insects could present a new opportunity to track and characterize the proteins synthetized by gut bacteria implicated in depolymerization of waste PE (Mohanan et al. 2020).

This study first examined the gut bacterial microbiome of *G. mellonella* larval stage for further microbiological investigations. From that it was assumed that a fraction of PE could disturb bacterial assemblages in *G. mellonella* gut. To test this hypothesis, the composition of the bacterial communities in two separate diets was characterized: wax moth larvae only feeding on standard (STD) diet (i.e., honeybee wax) and *G. mellonella* larvae feeding on co-diet mixing honeybee wax and PE. Finally, we screened the enzymes expressed by bacteria and discussed their pertinence and implications in PE biodegradation. Lastly, functional pathways of molecular determinants occurring in the microbiome and plastic degrading enzymes have been investigated based on proteomics.

## 2. Methods

### 2.1. Insect rearing and polyethylene diet

Rearing was initiated with a natural population of *G. mellonella* from Gembloux (Belgium). The identification of *G. mellonella* was morphologically confirmed (Ellis et al. 2013). Three glass containers of 80 L (Fig. S1A) with a wire mesh screen (1.5*1.5 mm) were set up for the source rearing mimicking the natural environment of *G. mellonella* into an hive and its frames are equipped with wax combs to feed the larvae (Metwally et al. 2012). Temperature and humidity rearing conditions were maintained at 30 ± 2°C and 70 ± 10% relative humidity (RH) in darkness (Ellis et al. 2013). Before the following experiment, two entire biological cycles elapsed (6-7 weeks) in these containers. From the source population, we selected 40 larvae aged between 25-35 days old (4-5 larval stage) (Jorjão et al. 2017), and dispatched them uniformly into eight 0.5 L meshed (1.5*1.5 mm) glass containers (Fig. S1B) (Hammer et al. 2015). Half of the 0.5 L meshed glass containers were provided with a ratio of polyethylene/honeybee wax (0.1 g: 2.8 g [w / w]) (Fig. S1C), with PE added as square of 1 cm * 1 cm. Additives free low-density polyethylene was purchased from GoodFellow (ET 311351, 300x300 mm and 0.23 mm thickness). The other containers were only provided with honeybee wax (control diet: 2.8 g). A quantity of 0.1 g of PE was selected with 2.8 g of wax to allow sufficient growth for 5 individuals. This co-diet supplementation ratio was selected to ensure the viability of 100% of the tested larvae (Bachynska et al. 2020). As soon as PE was totally ingested in 5-7 days, we selected two individuals per glass containers with weight more than 80 mg per 0.5 L glass container for dissection (n total = 16 caterpillars). We assumed that the ingestion of PE by the selected *G. mellonella* larvae from the 0.5 L containers is homogenous.

### 2.2. Sample collection and DNA and protein extraction

Larvae (n = 8 per diet) were starved for one hour before dissection. Under a laminar flow, larvae were rinsed with distilled water to discard fragments. Then they were surface-sterilized with ethanol 70% for 1 minute. The dissection was performed by immersing the whole body in 15 ml sterile PBS (NaCl 137 mM, KCl 2.7 mM, Na2HPO4 10 mM and KH2PO4 2 mM; pH: 7.4). Larvae were maintained on the ventral side and the incision was made at the final abdominal segment with sterile scissors and scalpels. Attention was paid to keep the gut tissue intact. Finally, the gut was cut through the proventricule in order to conserve the

midgut and hindgut (Fig. 1). Samples were then immediately transferred to a 1.5 ml sterile tube and frozen in liquid nitrogen (Shao et al. 2013). Each sample corresponds to a unique individual in order to reflect the individual midgut-hindgut bacterial microbiota. Next, disruption was done by crushing samples with sterile mortar and pestle. RLT lysis buffer (Qiagen, Hilden, Germany) was added before the homogenization step. Lysate was transferred to Qiashredder column (Qiagen, Hilden, Germany). Whole DNA and proteins were extracted by the ALLprep Kit (Qiagen, Hilden, Germany), following manufacturer instructions. DNA quality from *G. mellonella* larvae was checked by Nanodrop ND-1000 spectrophotometer (NanoDrop Technologies, Wilmington, DE, USA). Double stranded DNA quantity was determined by Qubit 2.0 (Quantitative dsDNA assay kit, Invitrogen, Carlsbad, California). DNA samples were kept at -20 °C until amplification.


**Fig. 1** Digestive tract (mouth: top right) of *G. mellonella* larva dissected on the ventral side. The foregut was discarded and the midgut-hindgut part was conserved for further DNA extraction.

For all the samples, the dry protein extract from the ALLprep assay of each sample was suspended in 100 µl of rehydration buffer (7 M urea, 2 M thio-urea, 0.5% (w:vol) CHAPS). The total protein concentration was quantified by the RC-DC protein assay kit (Biorad, USA). Twenty micrograms of protein was precipitated using the 2D Clean-up kit (GE, Healthcare). For each diet, four protein pellets were conserved at -80°C until further analyses.

### 2.3. 16S rRNA gene amplification by PCR

The polymerase chain reaction (PCR) amplification step was performed by targeting the V3-V4 hypervariable regions of the 16S ribosomal RNA gene of our 16 samples (n = 8 per diet). Primers S-D-Bact-0341-b-S-17/S-D-Bact-0785-a-A-21, with the Illumina™ (IDT, Iowa, USA) overhang adaptors at 5' were used (5 µM) (Klindworth et al. 2013). Briefly, KAPA HiFi Hot Start Ready Mix (12.5µl) (KAPA Biosystems, Wilmington, MA, USA) was used to amplify normalized DNA samples (2.5µl, 5ng/µl). The PCR cycle program was set up as follows in a thermal cycler: 1 cycle of denaturation during 3 min. at 95 °C, followed by a denaturation cycle of 25 times 30 sec. at 95°C, an annealing step at 55°C for 30 sec., then an elongation at 72°C during 30 sec. and finally, the extension was done at 72°C during 5 min. A second identical PCR was performed for samples with the control diet and four samples of the polyethylene diet to obtain enough DNA amplicons for further analysis.

### 2.4. Gene library preparation and sequencing of the 16S rRNA

Amplicon library was prepared for our 16 samples following the 16S metagenomic sequencing library preparation protocol (Illumina, San Diego, CA, USA). Purification was performed using AMPure XP system (Beckman Coulter Genomics, Brea, CA, USA). Then, index PCR was allowed by Nextera XT index Kit (Illumina, San Diego, CA, USA). Purification was performed again by AMPure XP bead beating. The library was checked for quality by Agilent 2200 Tape station (Agilent Technologies, Santa Clara, CA, USA). Then, the library was denatured by adding NaOH (0.2N) and the PhiX added. Finally, the library was sent to DNAvision (Belgium) for Illunina MiSeq 2x250 bp paired-end sequencing.

### 2.5. High-throughput sequencing data analysis

Subsequent processing of demultiplexed raw sequences was carried out using QIIME2 (Quantitative Insights Into Microbial Ecology; RRID:SCR_021258) version 2018.11 software (Bolyen et al. 2019). Reads were quality filtered (average min. score = 20), trimmed (F:17-245bp and R:21-245bp), de-noised, and merged thanks to DADA2 plug-in (Callahan et al. 2016), resulting in high resolution of amplicon sequence variants (ASVs) for downstream assessment. The plug-in q2-sample-classifier (Bokulich et al. 2018) was used to the taxonomy assignment using a naïve Bayesian classifier trained on the Greengenes reference database 13.8 with 97% similarity threshold. The ensuing ASVs table was filtered from mitochondria and chloroplasts before abundance visualization and analysis with R software

v3.6.3 (R Core Team 2020) and package *ggplot2* (Wickham 2009). Illumina Miseq sequencing of the V3-V4 region of the 16S rRNA gene generated a total of 1,225,244 reads across 16 samples from two diets (honeybee wax containing polyethylene or not), with a mean ± SD of 76,578 ± 21,867 unpaired sequences per sample. After quality filtering, 31,257 ± 9,175 unique sequences were conserved for the taxonomic assignation.

In order to reduce diversity overestimates, all ASVs present in a unique sample were discarded before standardized rarefaction at 15,000 reads with GUniFrac (Chen et al. 2012). To control for possible bias introduced by contaminants in our analyses, we applied a filtering threshold of 0.01% for low abundant ASVs as well as an additional filtering of ASVs present in less than 20% of samples. The alpha diversities were measured based on the Shannon index calculated with the *vegan* package (Oksanen et al. 2013). The effect of the diet on alpha diversity was assessed by a non-parametric Wilcoxon rank-sum test. We used the Aitchison distance (Aitchison 1986) to correct for compositional data and obtain a beta-diversity metric in an Euclidean space (pseudo-count of 1 added). We compared both diets (with polyethylene or not) by testing the null hypothesis that the centroids and dispersion of the groups were equal after permutational (1000 permutations) multivariate analysis of variance (PERMANOVA) with *adonis* function. Finally, to test for associations between the diet and the ASV abundances, we used a linear regression model after center-log ratio transformation (pseudo-count of 1 added). We kept a false discovery rate lower than 0.05 % for all reported p-values (Benjamini–Hochberg adjustment).

### 2.6. LC-ESI-MS/MS experiments

We randomly selected 8 samples (n = 4 per diet) from the 16 protein extractions (see point 2.2). Protein pellets were re-suspended in ammonium bicarbonate 50 mM, reduced using dithiotheotol, alkylated using iodoacetamide, and enzymatically digested using trypsin. The protein digests were purified on a Zip-Tip C18 before being injected in LC-MS/MS. The analysis was performed on an LC (Acquity UPLC Mclass – Waters) coupled with ESI-quadrupole orbitrap mass spectrometer (Q Exactive – Thermo Scientific), in positive ion mode. The obtained spectra were treated using Proteome Discoverer v.2.1 (Thermo Scientific). Identified peptides were aligned with protein sequences of NCBI Bacteria database, using the Sequest HT server. Carbamidomethyl of cysteines (resulting from alkylation before digestion) was set as a fixed modification. Oxidation of methionine and deamidation of asparagine and glutamine

were set as variable modifications. Trypsin cleavage rules were applied. The proteins were filtered with the following criteria: high FDR confidence and 1 or more unique peptides.

### 2.7. Proteomic analysis

Peak intensities were $log_2$-transformed and compared between PE and control diets. Only protein hits that were present in three out of the four replicates of each condition were taken into account for the following quantitative proteomic analyses. T-tests between the diets were performed, using a significant threshold of 0.05 and Benjamini-Hochberg FDR correction. Additionally, proteins were considered present in a condition only when they presented valid values for at least two out of the four replicates. Finally, proteins were considered as 'qualitatively differentially abundant proteins' when they presented valid values in at least two out of the replicates of one condition, and in none of the replicates of the other condition. Therefore, proteins that presented a valid value in only one of the replicates of at least one of the conditions could not be taken into account in this comparative study. The proteins were annotated using the software Blast2GO (BioBam, Spain; RRID:SCR_005828), regarding their molecular function and biological process (Götz et al. 2008).

## 3. Results

### 3.1. Taxonomic composition of the midgut-hindgut from *G. mellonella* larvae

The clustering of reads into ASV and their annotation using Greengenes database represented Firmicutes, Proteobacteria, and Actinobacteria as the three main phyla representing respectively 51 ± 26%, 43 ± 22% and 5 ± 3% % of the 107 ASVs identified after stringent filtering from the *G. mellonella* samples (mean ± sd). The average relative abundance of the families accounting for more than 1% is shown in Figure 2a. We identified *Enterococcaceae* and *Oxalobacteraceae* as the most abundant families whatever diet was provided. Considering the mean relative abundance for both diets, the analysis was able to identify ASVs belonging to *Enterococcus* as the main represented genus (49 ± 31 %). Then, *Curvibacter* (17 ± 10%) and the *Corynebacterium* (2 ± 1.5%) genera were among the most abundant (Fig. 2b).

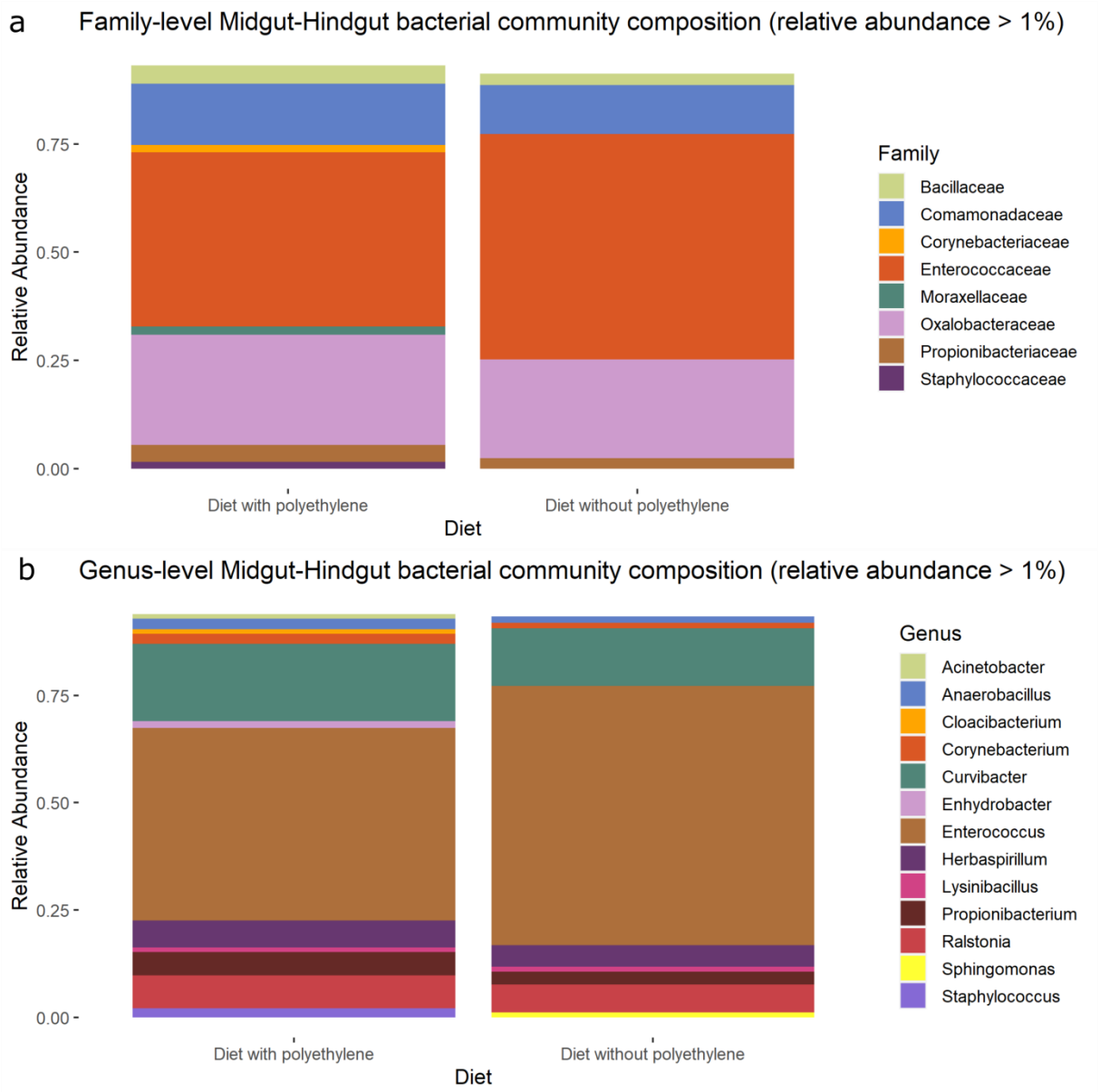


**Fig. 2** Taxonomic composition of the gut bacterial microbiome associated with the analyzed midgut-hindgut larval stages of *G. mellonella* at (a) family level and (b) genus level. Mean abundance was calculated for honeybee wax diet (8 samples) or honeybee wax plus polyethylene diet (8 samples). Only bacteria taxa with an average relative abundance higher than 1% are reported. The others belonged to minority taxa or were not assigned.

### 3.2. Co-diet supplementation on the gut bacterial microbiome

Considering the control diet (i.e. honeybee wax), the Firmicutes phylum was the most abundant (56 ± 24%). On the other hand, the Proteobacteria phylum accounted for the highest abundance (47 ± 25%) when polyethylene was present in the diet. Regarding the genus level, *Enterococcus* abundance was not significantly different between the control (57 ± 30 %) and the polyethylene diet (41 ± 33%) and *Corynebacterium* genus was neither significantly different for the diet with polyethylene (5 ± 0.06%) compared to the control (1 ± 1%).

Microbial diversities have been analyzed across both experimental diets. After removal of the low abundant ASVs (< 0.01 %), features present in less than 20% of the samples, and rarefaction to 15,000 sequences, the richness fell from 1,026 to 107 ASVs. The alpha-diversity index of the microbial community (Shannon's index) was not significantly different compared to both diets (Fig. 3). After controlling for compositional data structure by Aitchison transformation, we represented the variance explained by the first two eigenvectors in a principal component analysis (Fig. 4). We did not see any cluster explained by the diets. This observation was confirmed by PERMANOVA ($F = 1$, $p > 0.05$) where the null hypothesis was not rejected (similarity of centroids and/or dispersion of the population based on the diet). Indeed, the distance was not significantly different for the control than the polyethylene containing diet (PERMANOVA, $F = 1$, $p > 0.05$). Linear model regression was used to assess whether specific ASVs were associated with both diets. After a pseudo-count was added and abundances were center-log ratio transformed, bacterial composition in the samples from larval midgut-hindgut of *G. mellonella* differed poorly between the control and the polyethylene diet. As shown in the PCA (Fig. 4), the individual variability remains high across the population and could shade the effect of polyethylene on the gut bacterial microbiota.

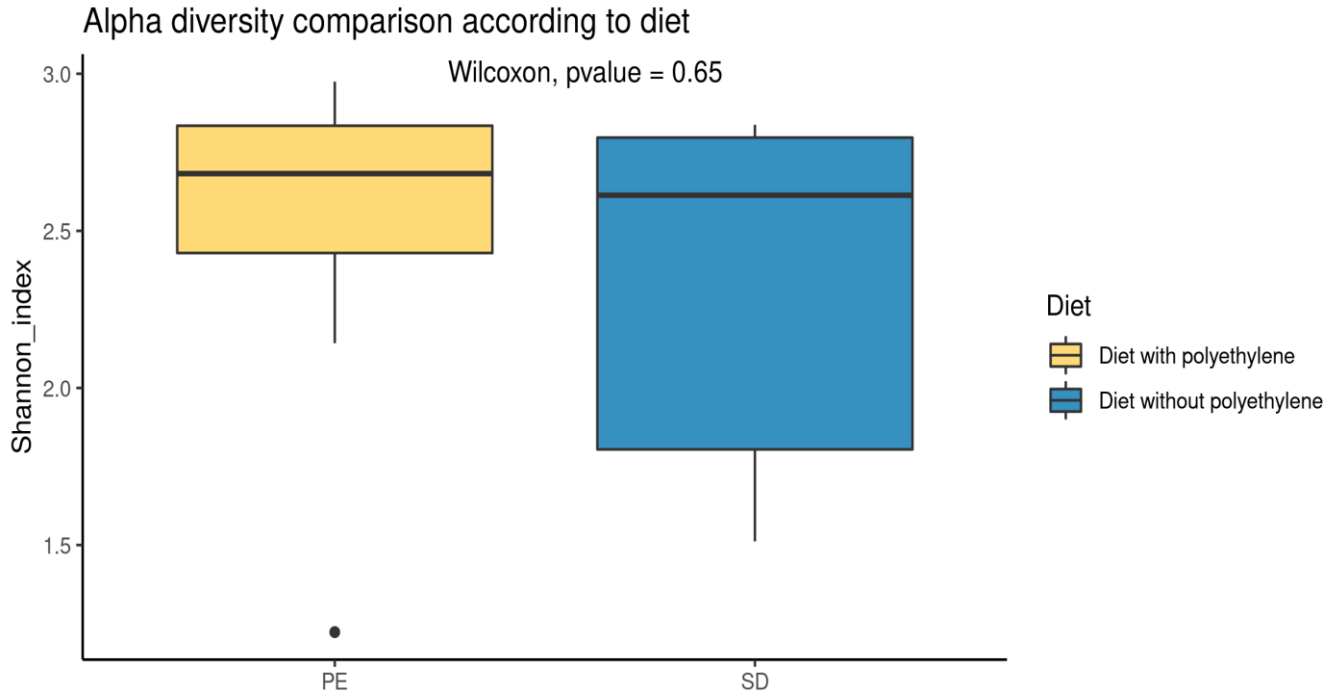


286 **Fig. 3** Shannon diversity index of the midgut-hindgut bacterial community from *G. mellonella* larval stages.
287 Comparison is made for diet containing only honeybee wax (8 samples) or honeybee wax plus polyethylene (8
288 samples). Rarefaction was set at 15,000 reads depth and ASVs <0.01% or present in less than 20% of the
289 samples were discarded. Statistical comparison of the two diets with the non-parametric test Wilcoxon-Mann-
290 Whitney was represented for comparison of the diets.

291

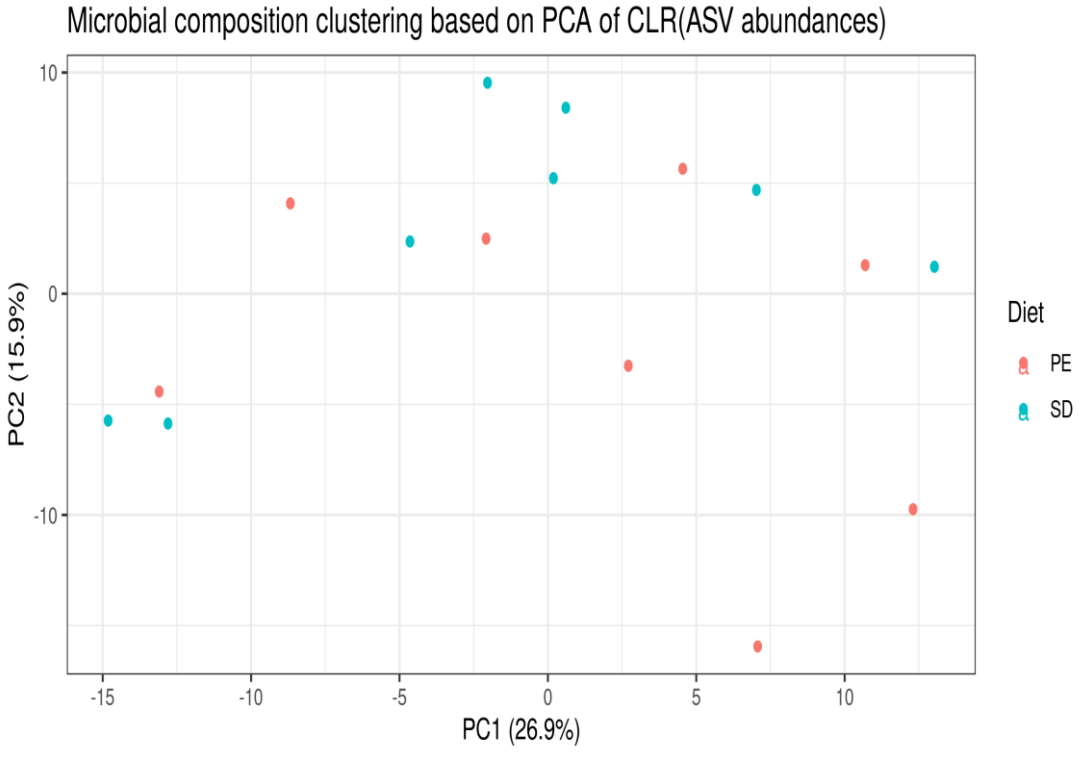

**Fig. 4** Principal Component Analysis (PCA) ordination based on the Aitchison transformed abundances (pseudo-count = 1) comparing the bacterial community from *G. mellonella* midgut-hindgut for the diet containing only honeybee wax (SD, blue) (8 samples) or honeybee wax plus polyethylene (PE, red) (8 samples).

### 3.3. Functional insight into the larval bacterial midgut-hindgut

In order to improve the current knowledge on the protein content of the larval gut, the gel-free quantitative proteomic analysis was carried out. Among the 55 identified proteins, 34 were considered in a comparative analysis between the diets of *G. mellonella* because they were present in all samples and are presented in Table 1. They were annotated according to their biological process, cellular component and molecular function (Fig. 5). No significant discrimination were observed in the proteome of PE-fed larvae, based on the control diet, but the proteins with a fold-change higher than 1.5 were highlighted in Table 1. Moreover, some bacteria-associated enzymes could be attributed to putative roles in plastic degradation such as phenylacetaldehyde dehydrogenase (Table 1).

**Table 1** LC-MS/MS analysis of the proteins content of the midgut-hindgut from *G. mellonella* larvae (n=4/diet). Labels highlighted in green correspond to proteins identified in a minimum of 2 samples per diet treatment (or in more than 2 samples and 0 for the other) and with a fold change > 1.5. Labels highlighted in orange correspond to proteins identified in a minimum of 2 samples of one diet treatment but only in one sample for the other diet and with a fold change > 1.5.

| Accession number | Description | OS | Score | MW [kDa] | calc. pI | Mean intensity (PE) | Mean intensity (Control) | Fold change based on control | Fold change based on PE | Mean Log2 Intensities (PE) | Mean log2 intensities (Control) | Putative role in plastic degradation ? |
|---|---|---|---|---|---|---|---|---|---|---|---|---|
| Q2G5N5 | ATP synthase subunit beta | Novosphingobium aromaticivorans (strain ATCC 700278 / DSM 12444 / CIP 105152 / NBRC 16084 / F199) | 60.49 | 51.1 | 5.0 | 230146050 | 245215735 | 0.94 | 1.07 | 27.72 | 27.87 | Not pertinent |
| Q4FP38 | ATP synthase subunit beta | Pelagibacter ubique (strain HTCC1062) | 54.29 | 50.7 | 5.0 | 241972661 | 149643964 | 1.62 | 0.62 | **27.75** | 26.71 | Not pertinent |
| Q28TJ6 | ATP synthase subunit beta | Jannaschia sp. (strain CCS1) | 51.12 | 50.5 | 4.7 | 235362059 | 284962555 | 0.83 | 1.21 | 27.74 | 28.02 | Not pertinent |
| Q7UM31 | Chaperone protein DnaK | Rhodopirellula baltica (strain DSM 10527 / NCIMB 13988 / SH1) | 37.72 | 69.4 | 4.7 | 316562445 | 455791588 | 0.69 | 1.44 | 28.18 | 28.73 | Not pertinent |
| Q0BQE8 | ATP synthase subunit beta | Granulibacter bethesdensis (strain ATCC BAA-1260 / CGDNIH1) | 37.42 | 51.2 | 5.1 | 71705264 | 70655416 | 1.01 | 0.99 | 26.01 | 26.03 | Not pertinent |
| A9M837 | ATP synthase subunit beta | Brucella canis (strain ATCC 23365 / NCTC 10854) | 35.30 | 54.8 | 5.7 | 123645823 | 126477814 | 0.98 | 1.02 | 26.66 | 26.84 | Not pertinent |
| Q2RFX9 | ATP synthase subunit beta | Moorella thermoacetica (strain ATCC 39073 / JCM 9320) | 25.84 | 50.4 | 5.1 | 95867523 | 157385134 | 0.61 | 1.64 | 26.45 | **27.18** | Not pertinent |
| B0THN2 | ATP synthase subunit beta | Heliobacterium modesticaldum (strain ATCC 51547 / Ice1) | 25.52 | 51.1 | 5.1 | 248989847 | 336066067 | 0.74 | 1.35 | 27.83 | 28.26 | Not pertinent |
| O66907 | ATP synthase subunit alpha | Aquifex aeolicus (strain VF5) | 22.89 | 55.5 | 5.3 | 138987578 | 166997178 | 0.83 | 1.20 | 27.03 | 27.23 | Not pertinent |
| B8FGT4 | ATP synthase subunit beta | Desulfatibacillum alkenivorans (strain AK-01) | 22.65 | 51.1 | 4.9 | 49358187 | 52479354 | 0.94 | 1.06 | 25.23 | 25.64 | Not pertinent |
| B9KPI6 | ATP synthase subunit alpha | Rhodobacter sphaeroides (strain KD131 / KCTC 12085) | 20.26 | 55.2 | 6.6 | 50490896 | 71562694 | 0.71 | 1.42 | 25.47 | 25.89 | Not pertinent |
| B8CXL1 | Chaperone protein DnaK | Halothermothrix orenii (strain H 168 / OCM 544 / DSM 9562) | 16.88 | 67.3 | 5.0 | 12047134 | 10907426 | 1.10 | 0.91 | 23.35 | 23.16 | Not pertinent |
| P49433 | Glyceraldehyde-3-phosphate dehydrogenase 1 | Synechocystis sp. (strain PCC 6803 / Kazusa) | 16.03 | 36.1 | 6.2 | 521396632 | 591746070 | 0.88 | 1.13 | 28.91 | 28.89 | Not pertinent |
| B8DYH6 | Chaperone protein DnaK | Dictyoglomus turgidum (strain Z-1310 / DSM 6724 | 15.25 | 66.9 | 5.7 | NA | 24575679 | NA | NA | NA | 24.25 | Not pertinent |
| Q98QY7 | Chaperone protein DnaK | Mycoplasma pulmonis (strain UAB CTIP) | 12.52 | 65.5 | 5.4 | 401868132 | 709128466 | 0.57 | 1.76 | 28.44 | **29.37** | Not pertinent |
| P31103 | Nucleoside diphosphate kinase | Bacillus subtilis (strain 168) | 9.12 | 16.9 | 5.9 | 325468131 | 312859317 | 1.04 | 0.96 | 28.23 | 28.12 | Not pertinent |
| B3EEQ2 | Enolase | Chlorobium limicola (strain DSM 245 / NBRC 103803 / 6330) | 8.47 | 46.9 | 5.1 | 335724525 | 391826337 | 0.86 | 1.17 | 28.29 | 28.31 | Not pertinent |
| B0SLC8 | ATP synthase subunit beta | Leptospira biflexa serovar Patoc (strain Patoc 1 / ATCC 23582 / Paris) | 7.36 | 51.1 | 5.4 | 74192057 | 102010329 | 0.73 | 1.37 | 26.08 | 26.58 | Not pertinent |
| Q89CK8 | Chaperone protein HtpG | Bradyrhizobium diazoefficiens (strain JCM 10833 / IAM 13628 / NBRC 14792 / USDA 110) | 6.66 | 68.9 | 5.2 | 218275841 | 223334750 | 0.98 | 1.02 | 27.63 | 27.70 | Not pertinent |
| Q6KIB0 | Enolase | Mycoplasma mobile (strain ATCC 43663 / 163K / NCTC 11711) | 5.64 | 49.8 | 6.3 | 27624064 | 46776753 | 0.59 | 1.69 | 24.72 | **25.37** | Not pertinent |
| P0A3J2 | Chaperone protein DnaK | Streptococcus agalactiae serotype III (strain NEM316) | 4.91 | 64.9 | 4.8 | 37280127 | 31141411 | 1.20 | 0.84 | 25.08 | 24.86 | Not pertinent |
| Q30YH6 | 60 kDa chaperonin | Desulfovibrio alaskensis (strain | 4.77 | 58.1 | 5.1 | 201351228 | 275191925 | 0.73 | 1.37 | 27.58 | 27.97 | Not pertinent |

| | | | | | | | | | | | | |
|---|---|---|---|---|---|---|---|---|---|---|---|---|
| | | G20) | | | | | | | | | | |
| Q89AG9 | 3-oxoacyl-[acyl-carrier-protein] reductase FabG | Buchnera aphidicola subsp. Baizongia pistaciae (strain Bp) | 4.47 | 26.8 | 10.1 | 114897914 | 94554169 | 1.22 | 0.82 | 26.66 | 26.21 | Not pertinent |
| A1ANS1 | Chaperone protein HtpG | Pelobacter propionicus (strain DSM 2379 / NBRC 103807 / OttBd1) | 4.35 | 73.9 | 5.1 | 179979890 | 120188761 | 1.50 | 0.67 | **27.34** | 26.74 | Not pertinent |
| A5WA09 | Adenosylhomocysteinase | Pseudomonas putida (strain ATCC 700007 / DSM 6899 / BCRC 17059 / F1) | 4.22 | 51.4 | 5.6 | 66925433 | 53510183 | 1.25 | 0.80 | 25.96 | 25.52 | Not pertinent |
| C5C3P2 | Chaperone protein DnaK | Beutenbergia cavernae (strain ATCC BAA-8 / DSM 12333 / NBRC 16432) | 3.01 | 66.9 | 4.8 | 49372303 | 76260132 | 0.65 | 1.54 | 25.54 | **26.08** | Not pertinent |
| O06837 | Phenylacetaldehyde dehydrogenase | Pseudomonas fluorescens | 2.64 | 53.5 | 5.8 | 696636494 | 495305880 | 1.41 | 0.71 | 29.10 | 28.13 | Pertinent |
| Q03YI2 | Elongation factor Tu | Leuconostoc mesenteroides subsp. mesenteroides (strain ATCC 8293 / NCDO 523) | 2.59 | 43.3 | 4.9 | 23713405 | 20478603 | 1.16 | 0.86 | 24.48 | 24.28 | Not pertinent |
| Q891P1 | V-type ATP synthase alpha chain 2 | Clostridium tetani (strain Massachusetts / E88) | 2.44 | 66.8 | 5.2 | 39280055 | 36460796 | 1.08 | 0.93 | 25.19 | 25.11 | Not pertinent |
| Q2G5Y5 | NADH-quinone oxidoreductase subunit C | Novosphingobium aromaticivorans (strain ATCC 700278 / DSM 12444 / CIP 105152 / NBRC 16084 / F199) | 2.23 | 34.1 | 5.1 | 22705457 | 18183835 | 1.25 | 0.80 | 24.39 | 24.11 | Not pertinent |
| Q2NA62 | NADH-quinone oxidoreductase subunit C | Erythrobacter litoralis (strain HTCC2594) | 2.23 | 28.1 | 4.5 | 22705457 | 18183835 | 1.25 | 0.80 | 24.39 | 24.11 | Not pertinent |
| Q2SMM8 | Chaperone protein DnaK | Hahella chejuensis (strain KCTC 2396) | 2.11 | 68.9 | 4.9 | 9527804 | 5036319 | 1.89 | 0.53 | **23.01** | 22.25 | Not pertinent |
| A5V9J6 | Phosphoglycerate kinase | Sphingomonas wittichii (strain RW1 / DSM 6014 / JCM 10273) | 1.29 | 41.4 | 5.4 | 20271133 | 49881216 | 0.41 | 2.46 | 24.27 | **25.55** | Not pertinent |
| A5FZU4 | Adenylate kinase | Acidiphilium cryptum (strain JF-5) | 1.18 | 24.0 | 6.4 | 29100592 | 72370266 | 0.40 | 2.49 | 24.76 | **26.11** | Not pertinent |

317

318

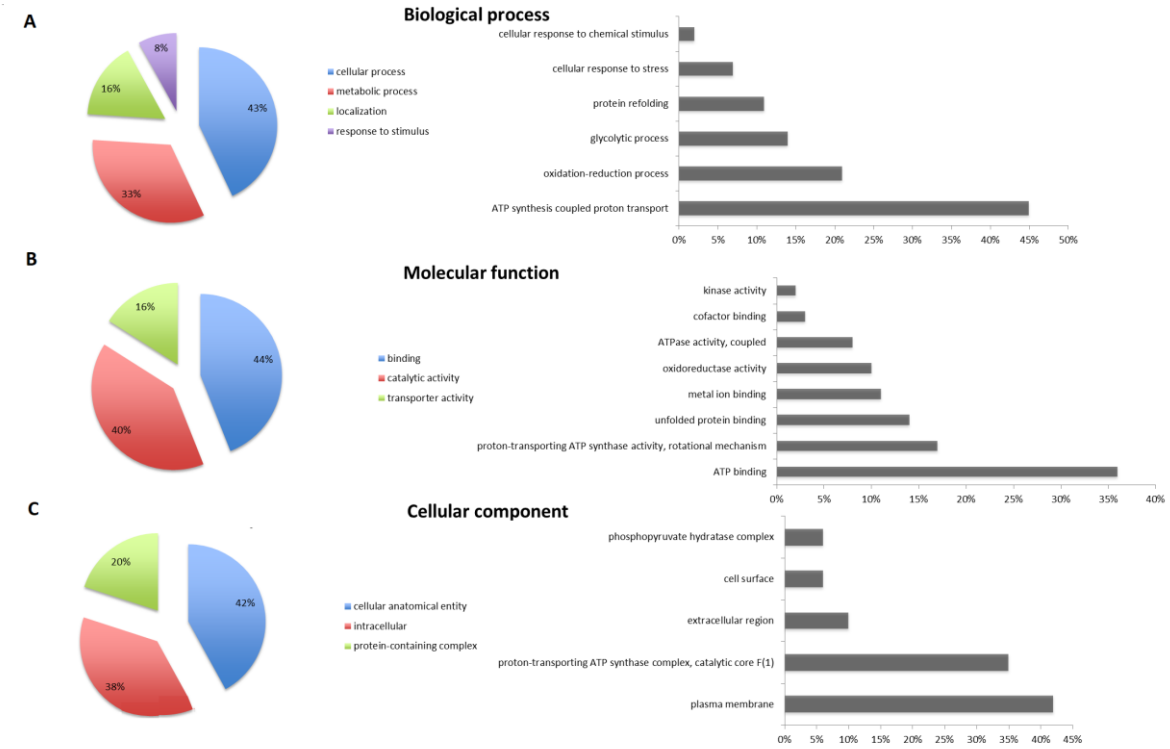


**Fig. 5** Summary of Blast2GO functional annotation of the identified proteins regarding their biological process (A), molecular function (B) and cellular component (C).

## 4. Discussion

In this study, we have investigated the bacterial midgut-hindgut microbial community of the greater wax moth (*G. mellonella*) larvae by sequencing the v3-v4 region of the 16s rRNA gene. We also have analyzed the exposition of wax-polyethylene diet on the taxonomic composition of the bacterial microbiome. This study was the first to combine a bacterial metagenomic and proteomic approach to the midgut-hindgut content of *G. mellonella* caterpillars.

### 4.1. Midgut-hindgut bacterial microbiome of *G. mellonella* share common insect gut pattern

The main genus present in the gut microbiome was widely shared by the Lepidoptera order. Indeed, *Enterococcus* represents the highest abundance for *Spodoptera littoralis* (Boisduval 1833), *Hyles euphorbiae* (L. 1758), *Brithys crini* (F. 1775), *Bombyx mori* (L. 1758) or the moth *Plutella xylostella* (L. 1758) (Fei et al. 2006; Tang et al. 2012; Vilanova et al. 2016; Li et al. 2017). The Enterococci were highlighted to dominate the *G. mellonella* larvae gut due to their ability to persist despite the replacement of the epithelium, the tolerance of a high pH, the ability to degrade a wide range of carbon sources and a

mutualism provided by the host (Johnston and Rolff 2015; Li et al. 2017; Liang et al. 2018). Previous studies on *G. mellonella* larvae gut observed more than 80% of *Enterococcus*, however, only the midgut part of the digestive tract was evaluated (Krams et al. 2017; Allonsius et al. 2019; Cassone et al. 2020). The large amount of ASVs part of the *Oxalobacteraceae* family was not identified in any previous study on the greater wax moth. Furthermore, these family members were commonly present in other insects gut microbiota like termites *Reticulitermes flavipes* (Kollar 1837) (Tarayre et al. 2015) or the sap-feeding herbivore *Mycopsylla fici* (Tryon 1895) (Fromont et al. 2017). Considering the bacterial richness of larval gut bacteria, *P. interpunctella* had higher observed OTUs. However, the diversity estimation by the Shannon's index (Fig. 3) was greater for *G. mellonella* suggesting a higher dominance-rarity effect of the bacterial assemblages (Mereghetti et al. 2017).

### 4.2. Co-diet supplementation on the gut bacterial microbiome

Other previous studies showed similar outcomes regarding to the alpha diversity metrics and the differential abundance analysis. Sole PE diet in Cassone et al., (2020) did not have the expected effect on the gut bacterial communities except an increased microbial abundance compared to caterpillars fed on honeybee wax. The used co-diet in this experiment did not provide an effect to favor certain taxa while the use of PE as sole diet can shape the larval core gut microbiome (Lou et al. 2020; Peydaei et al. 2021). This suggests that the bacterial microbiome of *G. mellonella* larvae could be resilient to bacterial community changes with 3-4% of PE diet co-supplementation. In fact, the chemical composition of PE being close to honeybee wax (Bombelli et al. 2017), which means that the gut bacterial communities are already adapted to degrade PE (Kong et al. 2019). For future research projects, a better standardization of the PE bioassays (e.g., PE ratio gradient, exposition time, larval weight or stage standardization…) and bioinformatics pipelines (e.g., FDR correction, classification strategy…) should be recommended to highlight changes in the bacterial community.

Also, we can point out some bacterial genera involving "plastic-eaters" bacteria such as *Corynebacterium* genus which are present in our wax moth gut samples. This genus is gram-positive bacilli belonging to *Corynebacteriaceae* and frequently present in the insect gut (Brandon et al. 2018). This genus was emphasized for its polyethylene degradation ability (Nowak et al. 2011). It should be interesting to deepen the identification of the gut microbiota at species level by metagenome assembled genomes

(MAGs) to infer the presence of these relevant degrading bacteria. Considering that diet can shape the bacterial gut community in insect populations (Colman et al. 2012), specific bacterial populations engaged in the digestion of PE could grow (e.g. *Corynebacterium* genus). Moreover, the *G. mellonella* gut epithelial cells are able to degrade long-chain hydrocarbons such as bees wax without the presence of its gut microbiome but need its assistance in the degradation of short-chain fatty acid (Kong et al. 2019; LeMoine et al. 2020).

### 4.3. Proteomics for functional insight of the bacterial midgut-hindgut proteome

According to the proteomic analysis based on the bacterial dataset reference, several proteins related to respiratory chain and energy metabolic pathway might be impacted by the addition of polyethylene in the honeybee wax diet. Firstly, ATP processes were identified, including several ATP synthases. A large multi-subunit enzyme complex converts the energy of oxidation-reduction reactions of the electron transport chain to the phosphorylation of ADP. The synthesis of ATP corresponds to the respiratory chain and represents the major cell energy source by the conversion into ADP to drive cellular functions (Xu et al. 2015). Changes in the energy metabolic pathway when changing the diets, such as including new carbon source here PE for *G. mellonella* larvae, are not surprising. Several enzymes associated with the protein folding in relation to the ATP binding molecular function were found to vary according to the plastic polymer included in the insect diet. A 60 kDa chaperonin and chaperone proteins DnaK were identified to change. Substrate binding and ATP hydrolysis by DnaK were found to be changed and are known to be regulated by chaperones (Genest et al. 2019). In particular, the DnaK substrates include unfolded, misfolded and aggregated proteins (Schlecht et al. 2011). The enzymatic cycle of DnaK alternates between ATP-bound open state and ADP-bound closed state (Mayer and Bukau 2005). Secondly, chaperone protein HtpG, known to display ATPase activity in cellular response to damages, was found to be deregulated in *G. mellonella* feeding on polyethylene diets.

Changes in the glycolytic process and energy metabolism were observed depending on the kind of diet including polyethylene. Indeed, ATP is generated from ADP in a number of metabolic reactions of glycolysis. A glycolytic enzyme, namely phosphoglycerate kinase (PGK) was changed with the insect diet. The PGK catalyzes the seventh step in glycolysis and is the first enzyme in the pathway to produce energy,

rather than consume it, by the creation of two molecules of ATP from the two molecules of 1,3-bisphospoglycerate produced from glucose in earlier steps (Bowler 2013).

Two enolases, well-known key glycolytic enzymes in the cytoplasm of prokaryotic and eukaryotic cells, were found to change according to the polyethylene occurrence in *G. mellonella* diet. Enolases are multifunctional proteins with key glycolytic roles that catalyze the switch of 2-phosphoglycerate to phosphoenolpyruvate, in the last steps of the catabolic glycolytic pathway (Díaz-Ramos et al. 2012). Finally, the styrene degradation process was identified in both diets of our insect model, *G. mellonella*. Indeed, phenylacetaldehyde dehydrogenase (PAD) is known to contribute to a side-chain oxygenation that has been reported as a specific route for the styrene degradation among microorganisms (Oelschlägel et al. 2018). Several studies revealed the attacks of the styrene vinyl-side chain are found to be a specific pathway for the styrene degradation for diverse organisms, leading to the formation of the central metabolite phenylacetic acid (Tischler 2015). Recently, Wang et al. (2022) proposed that the enzymes of *G. mellonella* supplemented by the enzymes from their gut bacteria can efficiently degrade polystyrene microplastics (PS). Two potential metabolic pathways have been proposed for the biodegradation of PS : the styrene oxide–phenylacetaldehyde and 4-methylphenol–4-hydroxybenzaldehyde–4-hydroxybenzoate pathways (Wang et al. 2022).

## 5. Conclusion

This study combined a deep identification of the taxonomic composition for the gut bacterial genome and proteome from *G. mellonella* larvae. Our experiment was able to show that the *Enterococcus* genus is widely abundant in the larval stage of the greater wax moth microbiome. According to the taxonomic composition, no bacterial community differences were observed between the diets. The functional analysis of insect gut content was promising for the identification of plastic degrading enzymes, such as PAD and should be deepened. Our works could provide valuable information for future plastic degradation studies. This finding, coupled with the identification of *Corynebacterium* bacteria genus related to plastic degradation, could have implications for discovery of potential enzymes produced by these candidate gut bacteria to degrade PE. Further investigation should be made on different polymers as well as on bacterial cultivation procedure.

417

# References


Aitchison J (1986) The statistical analysis of compositional data monographs on statistics and applied probability. Springer

Allonsius CN, Van Beeck W, De Boeck I, et al (2019) The microbiome of the invertebrate model host *Galleria mellonella* is dominated by *Enterococcus*. Anim Microbiome 1:1–7. https://doi.org/10.1186/s42523-019-0010-6

Amobonye A, Bhagwat P, Singh S, Pillai S (2021) Plastic biodegradation: Frontline microbes and their enzymes. Sci Total Environ 759:143536. https://doi.org/https://doi.org/10.1016/j.scitotenv.2020.143536

Bachynska YO, Markina TY, Lykova IO, Kharchenko LP (2020) Efficiency of using *Galleria mellonella* L. (Lepidoptera: Pyralidae) for waste processing of synthetic polymers. Biodivers Ecol Exp Biol 1:45–54. https://doi.org/10.34142/2708-5848.2020.22.1.05

Bokulich NA, Dillon M, Evan B, et al (2018) q2-sample-classifier: machine-learning tools for microbiome classification and regression. J open Res Softw 30:932. https://doi.org/10.21105/joss.00934

Bolyen E, Rideout JR, Dillon MR, et al (2019) Reproducible, interactive, scalable and extensible microbiome data science using QIIME 2. Nat Biotechnol 37:852–857. https://doi.org/10.1038/s41587-019-0209-9

Bombelli P, Howe CJ, Bertocchini F (2017) Polyethylene bio-degradation by caterpillars of the wax moth *Galleria mellonella* . Curr Biol 27:R292--R293. https://doi.org/10.1016/j.cub.2017.02.060

Bonhomme S, Cuer A, Delort AM, et al (2003) Environmental biodegradation of polyethylene. Polym Degrad Stab 81:441–452. https://doi.org/10.1016/S0141-3910(03)00129-0

Bowler MW (2013) Conformational dynamics in phosphoglycerate kinase, an open and shut case? FEBS Lett 587:1878–1883. https://doi.org/10.1016/j.febslet.2013.05.012

442 Brandon AM, Shu-Hong G, Renmao T, et al (2018) Biodegradation of polyethylene and plastic
443 mixtures in mealworms (larvae of *Tenebrio molitor*) and effects on the gut microbiome. Environ
444 Sci Technol 52:6526–6533. https://doi.org/10.1021/acs.est.8b02301

445 Callahan BJ, McMurdie PJ, Rosen MJ, et al (2016) DADA2: High-resolution sample inference from
446 Illumina amplicon data. Nat Methods 13:581–583. https://doi.org/10.1038/nmeth.3869

447 Carpenter EJ, Smith KLJ (1972) Plastics on the Sargasso Sea surface. Science (80- ) 175:1240–1241.
448 https://doi.org/10.1126/science.175.4027.1240

449 Cassone BJ, Grove HC, Elebute O, et al (2020) Role of the intestinal microbiome in low-density
450 polyethylene degradation by caterpillar larvae of the greater wax moth, *Galleria mellonella*. Proc
451 R Soc B Biol Sci 287:9–11. https://doi.org/10.1098/rspb.2020.0112

452 Chen J, Bittinger K, Charlson ES, et al (2012) Associating microbiome composition with
453 environmental covariates using generalized UniFrac distances. Bioinformatics 28:2106–2113.
454 https://doi.org/10.1093/bioinformatics/bts342

455 Colman DR, Toolson EC, Takacs-Vesbach CD (2012) Do diet and taxonomy influence insect gut
456 bacterial communities ? Mol Ecol 21:5124–5137. https://doi.org/10.1111/j.1365-
457 294X.2012.05752.x

458 Cook SM, McArthur JD (2013) Developing *Galleria mellonella* as a model host for human pathogens.
459 Virulence 4:350–353. https://doi.org/10.4161/viru.25240

460 Dadd RH (1966) Beeswax in the nutrition of the wax moth, *Galleria mellonella* (L.). J Insect Physiol
461 12:1479–1492. https://doi.org/https://doi.org/10.1016/0022-1910(66)90038-2

462 Díaz-Ramos À, Roig-Borrellas A, García-Melero A, López-Alemany R (2012) α-Enolase, a
463 multifunctional protein: Its role on pathophysiological situations. J Biomed Biotechnol
464 2012:156795. https://doi.org/10.1155/2012/156795

465 Dinh H, Semenec L, Kumar SS, et al (2021) Microbiology's next top model: *Galleria* in the molecular

age. Pathog Dis 79:1–11. https://doi.org/10.1093/femspd/ftab006

Ellis JD, Graham JR, Mortensen A (2013) Standard methods for wax moth research. J Apic Res 52:1–17. https://doi.org/10.3896/IBRA.1.52.1.10

Engel P, Moran NA (2013) The gut microbiota of insects - diversity in structure and function. FEMS Microbiol Rev 37:699–735. https://doi.org/10.1111/1574-6976.12025

Fei C, Lu X, Qian Y, et al (2006) Identification of Enterococcus sp. from midgut of silkworm based on biochemical and 16S rDNA sequencing analysis. Ann Microbiol 56:201–205. https://doi.org/10.1007/BF03175006

Fromont C, Riegler M, Cook JM (2017) Relative abundance and strain diversity in the bacterial endosymbiont community of a sap-feeding insect across its native and introduced geographic range. Microb Ecol 74:722–734. https://doi.org/10.1007/s00248-017-0971-5

Genest O, Wickner S, Doyle SM (2019) Hsp90 and Hsp70 chaperones: Collaborators in protein remodeling. J Biol Chem 294:2109–2120. https://doi.org/10.1074/jbc.REV118.002806

Ghatge S, Yang Y, Ahn J-H, Hur H-G (2020) Biodegradation of polyethylene: a brief review. Appl Biol Chem 63:27. https://doi.org/10.1186/s13765-020-00511-3

Götz S, García-Gómez JM, Terol J, et al (2008) High-throughput functional annotation and data mining with the Blast2GO suite. Nucleic Acids Res 36:3420–3435. https://doi.org/10.1093/nar/gkn176

Hammer TJ, Dickerson JC, Fierer N (2015) Evidence-based recommendations on storing and handling specimens for analyses of insect microbiota. PeerJ 3:e1190. https://doi.org/10.7717/peerj.1190

Johnston PR, Rolff J (2015) Host and symbiont jointly control gut microbiota during complete metamorphosis. PLoS Pathog 11:e1005246. https://doi.org/10.1371/journal.ppat.1005246

Jorjão AL, Oliveira LD, Scorzoni L, et al (2017) From moths to caterpillars: Ideal conditions for *Galleria mellonella* rearing for in vivo microbiological studies. Virulence 5594:0.

https://doi.org/10.1080/21505594.2017.1397871

Jovel J, Patterson J, Wang W, et al (2016) Characterization of the gut microbiome using 16S or shotgun metagenomics. Front Microbiol 7:1–17. https://doi.org/10.3389/fmicb.2016.00459

Klindworth A, Pruesse E, Schweer T, et al (2013) Evaluation of general 16S ribosomal RNA gene PCR primers for classical and next-generation sequencing-based diversity studies. Nucleic Acids Res 41:1–11. https://doi.org/10.1093/nar/gks808

Kong HG, Kim HH, Chung J hui, et al (2019) The *Galleria mellonella* hologenome supports microbiota-independent metabolism of long-chain hydrocarbon beeswax. Cell Rep 26:2451–2464. https://doi.org/10.1016/j.celrep.2019.02.018

Koutny M, Lemaire J, Delort AM (2006) Biodegradation of polyethylene films with prooxidant additives. Chemosphere 64:1243–1252. https://doi.org/10.1016/j.chemosphere.2005.12.060

Krams IA, Kecko S, Jõers P, et al (2017) Microbiome symbionts and diet diversity incur costs on the immune system of insect larvae. J Exp Biol 220:4204–4212. https://doi.org/10.1242/jeb.169227

Kumar Sen S, Raut S (2015) Microbial degradation of low density polyethylene (LDPE): A review. J Environ Chem Eng 3:462–473. https://doi.org/10.1016/j.jece.2015.01.003

Kundungal H, Gangarapu M, Sarangapani S, et al (2021) Role of pretreatment and evidence for the enhanced biodegradation and mineralization of low-density polyethylene films by greater waxworm. Environ Technol 42:717–730. https://doi.org/10.1080/09593330.2019.1643925

Kundungal H, Gangarapu M, Sarangapani S, et al (2019) Efficient biodegradation of polyethylene (HDPE) waste by the plastic-eating lesser waxworm (*Achroia grisella*). Environ Sci Pollut Res 26:18509–18519. https://doi.org/10.1007/s11356-019-05038-9

Kwadha CA, Ong'Amo GO, Ndegwa PN, et al (2017) The biology and control of the greater wax moth, *Galleria mellonella*. Insects 8:1–17. https://doi.org/10.3390/insects8020061

LeMoine CMR, Grove HC, Smith CM, Cassone BJ (2020) A very hungry caterpillar: Polyethylene

metabolism and lipid homeostasis in larvae of the greater wax moth (*Galleria mellonella*). Environ Sci Technol 54:14706–14715. https://doi.org/10.1021/acs.est.0c04386

Li W, Jin D, Shi C, Li F (2017) Midgut bacteria in deltamethrin-resistant, deltamethrin-susceptible, and field-caught populations of *Plutella xylostella*, and phenomics of the predominant midgut bacterium *Enterococcus mundtii*. Sci Rep 7:1–13. https://doi.org/10.1038/s41598-017-02138-9

Li WC, Tse HF, Fok L (2016) Plastic waste in the marine environment: A review of sources, occurrence and effects. Sci Total Environ 566–567:333–349. https://doi.org/10.1016/j.scitotenv.2016.05.084

Liang X, Sun C, Chen B, et al (2018) Insect symbionts as valuable grist for the biotechnological mill : an alkaliphilic silkworm gut bacterium for efficient lactic acid production. Appl Microbiol Biotechnol 102:4951–4962

Lou Y, Ekaterina P, Yang S-S, et al (2020) Biodegradation of polyethylene and polystyrene by greater wax moth larvae (*Galleria mellonella* L.) and the effect of co-diet supplementation on the core gut microbiome. Environ Sci Technol 54:2821–2831. https://doi.org/10.1021/acs.est.9b07044

Mayer MP, Bukau B (2005) Hsp70 chaperones: cellular functions and molecular mechanism. Cell Mol Life Sci 62:670–684. https://doi.org/10.1007/s00018-004-4464-6

Mereghetti V, Chouaia B, Limonta L, et al (2017) Evidence for a conserved microbiota across the different developmental stages of *Plodia interpunctella*. Insect Sci 26:466–478. https://doi.org/10.1111/1744-7917.12551

Metwally HMS, Hafez GA, Hussein MA, et al (2012) Low cost artificial diet for rearing the greater wax moth , *Galleria mellonella* L . ( Lepidoptera : Pyralidae ) as a host for entomopathogenic nematodes. Egypt J Pest Control 22:15–17

Mohanan N, Montazer Z, Sharma PK, Levin DB (2020) Microbial and enzymatic degradation of synthetic plastics. Front Microbiol 11:580709. https://doi.org/10.3389/fmicb.2020.580709

538 Montazer Z, Habibi Najafi MB, Levin D (2020) In vitro degradation of low-density polyethylene by
539 new bacteria from larvae of the greater wax moth, *Galleria mellonella*. Can J Microbiol 67:1–10.
540 https://doi.org/10.1139/cjm-2020-0208

541 Nowak B, Pajak J, Drozd-Bratkowicz M, Rymarz G (2011) Microorganisms participating in the
542 biodegradation of modified polyethylene films in different soils under laboratory conditions. Int
543 Biodeterior Biodegrad 65:757–767. https://doi.org/10.1016/j.ibiod.2011.04.007

544 Oberbeckmann S, Osborn AM, Duhaime MB (2016) Microbes on a bottle: Substrate, season and
545 geography influence community composition of microbes colonizing marine plastic debris. PLoS
546 One 11:1–24. https://doi.org/10.1371/journal.pone.0159289

547 Oelschlägel M, Zimmerling J, Tischler D (2018) A review: The styrene metabolizing cascade of side-
548 chain oxygenation as biotechnological basis to gain various valuable compounds. Front
549 Microbiol 9:1–17. https://doi.org/10.3389/fmicb.2018.00490

550 Ojha N, Pradhan N, Singh S, et al (2017) Evaluation of HDPE and LDPE degradation by fungus,
551 implemented by statistical optimization. Sci Rep 7:1–13. https://doi.org/10.1038/srep39515

552 Oksanen AJ, Blanchet FG, Kindt R, et al (2013) Package ‘ vegan ’ version 2.5-2

553 Petriz BA, Franco OL (2017) Metaproteomics as a complementary approach to gut microbiota in
554 health and disease. Front Chem 5:1–7. https://doi.org/10.3389/fchem.2017.00004

555 Peydaei A, Bagheri H, Gurevich L, et al (2020) Impact of polyethylene on salivary glands proteome in
556 *Galleria melonella*. Comp Biochem Physiol Part D Genomics Proteomics 34:100678.
557 https://doi.org/https://doi.org/10.1016/j.cbd.2020.100678

558 Peydaei A, Bagheri H, Gurevich L, et al (2021) Mastication of polyolefins alters the microbial
559 composition in *Galleria mellonella*. Environ Pollut 280:116877.
560 https://doi.org/https://doi.org/10.1016/j.envpol.2021.116877

561 Pivato AF, Miranda GM, Prichula J, et al (2022) Hydrocarbon-based plastics: Progress and

562 perspectives on consumption and biodegradation by insect larvae. Chemosphere 293:133600.
563 https://doi.org/10.1016/j.chemosphere.2022.133600

564 Plastics Europe (2021) Plastics – the Facts 2021. https://plasticseurope.org/wp-
565 content/uploads/2021/12/Plastics-the-Facts-2021-web-final.pdf (Lastly consulted on 15
566 November 2022)

567 R Core Team (2020) R: A language and environment for statistical computing. https://www.r-
568 project.org/ (Lastly consulted on 15 November 2022)

569 Ruiz Barrionuevo JM, Vilanova-Cuevas B, Alvarez A, et al (2022) The Bacterial and Fungal Gut
570 Microbiota of the Greater Wax Moth, Galleria mellonella L. Consuming Polyethylene and
571 Polystyrene. Front Microbiol 13:918861. https://doi.org/10.3389/fmicb.2022.918861

572 Sanchez-Hernandez JC (2021) A toxicological perspective of plastic biodegradation by insect larvae.
573 Comp Biochem Physiol Part C Toxicol Pharmacol 248:109117.
574 https://doi.org/https://doi.org/10.1016/j.cbpc.2021.109117

575 Schlecht R, Erbse AH, Bukau B, Mayer MP (2011) Mechanics of Hsp70 chaperones enables
576 differential interaction with client proteins. Nat Struct Mol Biol 18:345–351.
577 https://doi.org/10.1038/nsmb.2006

578 Shao Y, Arias-Cordero EM, Boland W (2013) Identification of metabolically active bacteria in the gut
579 of the generalist *Spodoptera littoralis* via DNA stable isotope probing using 13C-Glucose. J Vis
580 Exp 1–8. https://doi.org/10.3791/50734

581 Shimao M (2001) Biodegradation of plastics. Curr Opin Biotechnol 12:242–247.
582 https://doi.org/10.1016/S0958-1669(00)00206-8

583 Stefanini I (2018) Yeast-insect associations: it takes guts. Yeast. https://doi.org/10.1002/yea.3309

584 Sugeçti S (2021a) Pathophysiological effects of *Klebsiella pneumoniae* infection on *Galleria*
585 *mellonella* as an invertebrate model organism. Arch Microbiol 203:3509–3517.

https://doi.org/10.1007/s00203-021-02346-y

Sugeçti S (2021b) Biochemical and immune responses of model organism *Galleria mellonella* after infection with *Escherichia coli*. Entomol Exp Appl 169:911–917. https://doi.org/10.1111/eea.13092

Tang X, Freitak D, Vogel H, et al (2012) Complexity and variability of gut commensal microbiota in polyphagous lepidopteran larvae. PLoS One 7:1–9. https://doi.org/10.1371/journal.pone.0036978

Tarayre C, Bauwens J, Mattéotti C, et al (2015) Multiple analyses of microbial communities applied to the gut of the wood-feeding termite *Reticulitermes flavipes* fed on artificial diets. Symbiosis 65:143–155. https://doi.org/10.1007/s13199-015-0328-0

Tischler D (2015) Microbial Styrene Degradation, 1st edn. Springer International Publishing

Vilanova C, Baixeras J, Latorre A, Porcar M (2016) The generalist inside the specialist: Gut bacterial communities of two insect species feeding on toxic plants are dominated by *Enterococcus* sp. Front Microbiol 7:1–8. https://doi.org/10.3389/fmicb.2016.01005

Wang S, Shi W, Huang Z, et al (2022) Complete digestion/biodegradation of polystyrene microplastics by greater wax moth (*Galleria mellonella*) larvae: Direct in vivo evidence, gut microbiota independence, and potential metabolic pathways. J Hazard Mater 423:127213. https://doi.org/https://doi.org/10.1016/j.jhazmat.2021.127213

Warnecke F, Luginbühl P, Ivanova N, et al (2007) Metagenomic and functional analysis of hindgut microbiota of a wood-feeding higher termite. Nature 450:560–565. https://doi.org/10.1038/nature06269

Wickham H (2009) ggplot2: Elegant Graphics for Data Analysis. Biometrics 67:678–679. https://doi.org/10.1111/j.1541-0420.2011.01616.x

Xu T, Pagadala V, Mueller DM (2015) Understanding structure, function, and mutations in the mitochondrial ATP synthase. Microb Cell 2:105–125. https://doi.org/10.15698/mic2015.04.197

610 Yang J, Yang Y, Wu WM, et al (2014) Evidence of polyethylene biodegradation by bacterial strains
611 from the guts of plastic-eating waxworms. Environ Sci Technol 48:13776–13784.
612 https://doi.org/10.1021/es504038a

613 Yang Y, Yang J, Wu WM, et al (2015) Biodegradation and Mineralization of Polystyrene by Plastic-
614 Eating Mealworms: Part 2. Role of Gut Microorganisms. Environ Sci Technol 49:12087–12093.
615 https://doi.org/10.1021/acs.est.5b02663

616 Zhu P, Pan X, Li X, et al (2021) Biodegradation of plastics from waste electrical and electronic
617 equipment by greater wax moth larvae (*Galleria mellonella*). J Clean Prod 310:127346.
618 https://doi.org/https://doi.org/10.1016/j.jclepro.2021.127346

619

## Statements & Declarations

### Funding

This work was supported by internal resources.

### Competing interests

The authors declare that they have no competing interests.

### Authors' contributions

GN performed the sampling and the rearing of *Galleria mellonella*. SM, FD and FF conceived the study and provided the financial support. LS and ARS did the laboratory work. GN and LS analyzed the data and interpreted the results. GN wrote the first draft complemented by LS and FF. All the authors were involved in the writing process (review and editing).

### Ethics approval

Not applicable.

### Consent to participate

Not applicable.

### Consent to publish

Not applicable.

### Data Availability

The sequencing data have been deposited with links to BioProject accession number PRJNA730794 in the NCBI BioProject database (https://www.ncbi.nlm.nih.gov/bioproject/). The mass spectrometry proteomics data have been deposited to the ProteomeXchange Consortium via the PRIDE partner repository with the dataset identifier PXD026446.

### Code Availability

Not applicable.

644